Published for SISSA by Springer

Received: October 10, 2022
Revised: March 1, 2023
Accepted: March 13, 2023
Published: March 27, 2023

Holographic imaginary potential of a quark antiquark pair in the presence of gluon condensation

JHEP03(2023)207

Sara Tahery,[a] **Xurong Chen**[a,b] **and Zi-qiang Zhang**[c]

[a] *Institute of Modern Physics, Chinese Academy of Sciences, Lanzhou 730000, China*
[b] *University of Chinese Academy of Sciences, Beijing 100049, China*
[c] *School of Mathematics and Physics, China University of Geosciences, Wuhan 430074, China*

E-mail: s.tahery@impcas.ac.cn, xchen@impcas.ac.cn, zhangzq@cug.edu.cn

Abstract: For a moving heavy quark antiquark ($Q\bar{Q}$) in a quark gluon plasma (QGP), we use gauge/gravity duality to study both real and imaginary parts of the potential ($\mathrm{Re}V_{Q\bar{Q}}$ and $\mathrm{Im}V_{Q\bar{Q}}$ respectively) in a gluon condensate (GC) theory. The complex potential is derived from the Wilson loop by considering the thermal fluctuations of the worldsheet of the Nambu-Goto holographic string. We calculate $\mathrm{Re}V_{Q\bar{Q}}$ and $\mathrm{Im}V_{Q\bar{Q}}$ in both cases where the axis of the moving $Q\bar{Q}$ pair is transverse and parallel with respect to its direction of movement in the plasma. Using the renormalization scheme for the $\mathrm{Re}V_{Q\bar{Q}}$, we find that the inclusion of GC increases the dissociation length while rapidity has the opposite effect. While for the $\mathrm{Im}V_{Q\bar{Q}}$, we observe that by considering the effect of GC, the $\mathrm{Im}V_{Q\bar{Q}}$ is generated for larger distance thus decreasing quarkonium dissociation, while rapidity has opposite effect. In particular, as the value of GC decreases in the deconfined phase, the $\mathrm{Im}V_{Q\bar{Q}}$ is generated for smaller distance thus enhancing quarkonium dissociation, and at high temperatures it is nearly not modified by GC, consistent with previous findings of the entropic force.

Keywords: AdS-CFT Correspondence, Gauge-Gravity Correspondence, Quark-Gluon Plasma

ArXiv ePrint: 2208.01233

https://doi.org/10.1007/JHEP03(2023)207

Contents

1 Introduction

The heavy ion collisions at Relativistic Heavy Ion Collisions (RHIC) and Large Hadron Collider (LHC) have produced a new state of matter called QGP [1–3]. One of the most experimental signatures of QGP formation is the dissociation of quarkonia, like $c\bar{c}$ in the medium [4–8]. Most studies over the past years have found that the main mechanism responsible for this dissociation is color screening [9], however, recent studies suggest a more important reason than the screening, the $\mathrm{Im}V_{Q\bar{Q}}$ [10]. Moreover, this quantity could be used to estimate the thermal width which is an important subject in QGP [11, 12]. Calculations of the $\mathrm{Im}V_{Q\bar{Q}}$ associated with QCD and heavy ion collisions were performed for static pairs using pQCD [13, 14]. However, theoretical analysis and experimental data demonstrate that QGP is strongly coupled [15], then non-perturbative methods are needed. The equation of state of the QGP at zero and finite temperature are given in [16, 17] and the $\mathrm{Im}V_{Q\bar{Q}}$ was studied in [18–20] by using non-perturbative lattice QCD. Note that lattice QCD is very useful but still very difficult to use to study real-time QCD dynamics. An alternative method to study different aspects of QGP is the AdS/CFT correspondence.

AdS/CFT conjecture originally relates the type IIB string theory on $AdS_5 \times S^5$ space-time to the four-dimensional $\mathcal{N} = 4$ SYM gauge theory [21]. In a holographic description of AdS/CFT, a strongly coupled field theory at the boundary of the AdS space is mapped onto the weakly coupled gravitational theory in the bulk of AdS [22]. Although SYM differs from QCD in many properties (e.g., at zero temperatures, SYM is a conformal theory with no particle spectrum while QCD is a confining theory with a sensible particle interpretation), it reveals some qualitative features of QCD in strongly coupled regime at non-zero temperatures (e.g., both theories describe hot, non-Abelian plasmas with qualitatively similar hydrodynamic behavior [23]). Given that, one could use the AdS/CFT correspondence to study various aspects of QGP. An example of the most known AdS/CFT calculations is the ratio of shear viscosity to entropy density [23, 24].

JHEP03(2023)207

On the other hand, the AdS/CFT correspondence has been generalized to more realistic QCD, e.g, bottom-up holographic model [25, 26]. The bottom-up approach begins with a five-dimensional effective field theory somehow motivated by string theory and tries to fit it to QCD as much as possible. In the gravitational dual of QCD, the presence of probe branes in the AdS bulk breaks the conformal symmetry and sets the energy scales, so corrections in AdS_5 are useful to find more phenomenological results. Holographic GC model [27–29] is a type of bottom-up model with phenomenological applicability as an effective model for the QGP. It is known that GC is a measure of the non-perturbative physics in zero-temperature QCD [30], it is also an order parameter for (de)confinement hence could be a condition for the phase transition (the usual order parameter for the deconfinement transition at finite temperature is the Polyakov loop. Also the Wilson loop can be used to identify the (de)confined phases of pure YM theory by its area law behavior). Although there is no order parameter for the real-world QGP, GC model may be useful to study the nonperturbative nature of the QGP [31–40], such as in RHIC physics [41]. In the mentioned references it is shown that QCD sum rules is used to study the nonperturbative physics of the strong interaction at zero temperature. In this approach, the nonperturbative nature of the vacuum is summarized in terms of quark and gluon condensates. To study hot systems, one generalizes the technique to finite temperature. The non-perturbative physics remaining even at high temperatures, is manifested through the non-vanishing of some of the vacuum condensates. Furthermore, using the GC model, the thermodynamic properties of the system are discussed in [31], in which the well-known Stephan-Boltzmann law with no condensation case can be recovered, also the energy density for high temperature is given but for low temperature other back ground is dominating. In the same reference, the dilaton (or GC) contribution of the energy momentum tensor is identified as the difference of the total and the thermal gluon, the GC contributes negative energy which is a reminiscent of the zero temperature result of Shifman, Vainstein and Zakharov [30]. In both cases, the negativeness is coming from the renormalization. Also in [31] the pressure, the trace anomaly and the entropy density are given in presence of GC, as it is expected, the entropy in condensed state is less than that in thermal state. On the other hand, various observables or quantities have been studied in Holographic GC model. For instance, the GC dependency of the heavy quark potential was studied in [42] and the results indicate that the potential becomes deeper as the GC in the deconfined phase decreases and the mass of the quarkonium drops near the deconfinement temperature T_c (lattice QCD results [43, 44] show that the GC appears a drastic change near T_c). The GC dependency of the jet quenching parameter and drag force was analyzed in [45] and it was found that the two quantities both decrease as the GC decreases in the deconfined phase, indicating that the energy loss decreases near T_c. In [46] it is shown that the dropping GC near T_c increases the entropic force and thus enhances the quarkonium dissociation.

The aim of this work is to analyze the $\mathrm{Im}V_{Q\bar{Q}}$ of moving $Q\bar{Q}$ in holographic GC model using the world-sheet thermal fluctuations method [47–49]. Note that the effect of the medium in the motion of a $Q\bar{Q}$ should be taken into account and the pair's rapidity through the plasma has some effects on their interactions. In the LHC, the heavy quarkonia are not only produced in large numbers but also with high momenta so it is essential to consider the effect of bound state speed on dissociation [50]. As discussed in [49], one can adopt the saddle point approximation and discuss the motion of a heavy quarkonia in a plasma and its imaginary potential. The imaginary potential of the $Q\bar{Q}$ results from the effect of thermal fluctuations due to the interactions between quarks and the strongly coupled medium. By integrating out thermal long wavelength fluctuations in the path integral of the Nambu-Goto action in the background spacetime, a formula for the imaginary part of the Wilson loop can be found in this approach that is valid for any gauge theory dual to classical gravity. Already, different holographic models were applied to study the $\mathrm{Im}V_{Q\bar{Q}}$ of the $Q\bar{Q}$ [25, 51–72]. It is worth to mention that in [49] the $\mathrm{Im}V_{Q\bar{Q}}$ of moving $Q\bar{Q}$ is considered in strongly coupled plasma (associated with pure AdS), while in this work we extend it to the AdS with GC. In [51] the $\mathrm{Im}V_{Q\bar{Q}}$ of moving $Q\bar{Q}$ in OKS model (a type of holographic model) is discussed, by delving into the solution beyond the critical separation of the pair, which leads to the complex-valued string configurations, not the world-sheet thermal fluctuations method as we use here. In [52] the $\mathrm{Im}V_{Q\bar{Q}}$ of moving $Q\bar{Q}$ in a soft wall model with broken conformal invariance and finite chemical potential is discussed. As holographic examples, such as [49, 51–53] and [60] considered the moving cases, and they concluded that increasing rapidity leads to decreasing the dissociation length, implying the pair will be dissolved easier into a moving medium compared to the static medium, consistent with our findings here. However, from EFT point of view, the reference [73] explored the in-medium modifications of heavy quarkonium states moving through a medium for two plausible situations: $m_Q \gg 1/r \gg T \gg E \gg m_D$ and $m_Q \gg T \gg 1/r, m_D \gg E$, results are relevant for moderate temperatures and for studying dissociation, respectively. The width decreases with the velocity for the former situation whereas for the latter regime the width increases monotonically with the velocity.

This paper is organized as follows: in the next section we study the $\mathrm{Re}V_{Q\bar{Q}}$ for both cases in which the dipole moves transversely and parallel to the dipole axis. We proceed to calculate the $\mathrm{Im}V_{Q\bar{Q}}$ for the two cases mentioned in the section 3. Section 4 contains results and conclusions.

2 Potential of moving $Q\bar{Q}$ in presence of gluon condensation

In this section we evaluate the $\mathrm{Re}V_{Q\bar{Q}}$ of the moving $Q\bar{Q}$. The heavy quark potential (the vacuum interaction energy) is related to the vacuum expectation value of the Wilson loop [74–76] as,

$$\lim_{\mathcal{T}\longrightarrow 0} \langle W(\mathcal{C})\rangle_0 \sim e^{i\mathcal{T}V_{Q\bar{Q}}(L)}, \tag{2.1}$$

where $\mathcal{C}$ is a rectangular loop of spatial length L and extended over $\mathcal{T}$ in the time direction. The expectation value of the Wilson loop can be evaluated in a thermal state of the gauge theory with the temperature T. From this point of view $V_{Q\bar{Q}}(L)$ is the heavy quark potential at finite temperature and its imaginary part defines a thermal decay width. To estimate the $\mathrm{Im}V_{Q\bar{Q}}$ mentioned, one can use worldsheet fluctuations of the Nambu-Goto action [47].

Note that although the Nambu-Goto action on top of a background with a non-trivial dilaton field contains a coupling of this field with the Ricci scalar as it is shown in [77], but the contribution of this term is small. Therefore the well-known modified holographic model introducing the GC in the boundary theory is given by the following background action,

$$S = -\frac{1}{2k^2}\int d^5x\sqrt{g}\left(\mathcal{R} + \frac{12}{R^2} - \frac{1}{2}\partial_\lambda\varphi\partial^\lambda\varphi\right), \tag{2.2}$$

where k is the gravitational coupling in 5-dimensions, $\mathcal{R}$ is Ricci scalar, R is the radius of the asymptotic AdS_5 spacetime, and φ is a massless scalar which is coupled with the gluon operator on the boundary. By considering the following ansatz the equations of the above action could be solved [27–29],

$$ds^2 = \frac{R^2}{z^2}\left(A(z)dx_i^2 - B(z)dt^2 + dz^2\right), \tag{2.3}$$

where in this dilaton black hole background, $A(z), B(z), f$ are defined as,

$$\begin{aligned} A(z) &= (1+fz^4)^{\frac{f+a}{2f}}(1-fz^4)^{\frac{f-a}{2f}}, \\ B(z) &= (1+fz^4)^{\frac{f-3a}{2f}}(1-fz^4)^{\frac{f+3a}{2f}}, \\ f^2 &= a^2 + c^2, \end{aligned} \tag{2.4}$$

a is related to the temperature by $a = \frac{(\pi T)^4}{4}$ and the dilaton field is given by,

$$\phi(z) = \frac{c}{f}\sqrt{\frac{3}{2}}\ln\frac{1+fz^4}{1-fz^4} + \phi_0. \tag{2.5}$$

In (2.3) $i = 1, 2, 3$ are orthogonal spatial boundary coordinates, z denotes the 5th dimension, radial coordinate and $z = 0$ sets the boundary. ϕ_0 in (2.5) is a constant. We work in the unit where $R = 1$. Note that the dilaton black hole solution is well defined only in the range $0 < z < f^{-1/4}$, where f determines the position of the singularity and z_f behaves as an IR cutoff. For $a = 0$, it reduces to the dilaton-wall solution. Meanwhile, for $c = 0$, it becomes the Schwarzschild black hole solution. Also, for both solutions, expanding the dilaton profile near $z = 0$ will give,

$$\phi(z) = \phi_0 + \sqrt{6}\,c\,z^4 + \dots \tag{2.6}$$

c is nothing but the holographic GC parameter. As discussed in [31], there exists a Hawking page transition between the dilaton wall solution and dilaton blackhole solution at some critical value of a. So the former is for the confined phase, while the latter describes the deconfined phase. The term G_2 is the vacuum expectation value of the operator $\frac{\alpha_s}{\pi}G^a_{\mu\nu}G^{a,\mu\nu}$ where $G^a_{\mu\nu}$ is the gluon field strength tensor. A non-zero trace of the energy-momentum tensor appears in a full quantum theory of QCD. The anomaly implies a non-zero GC which can be calculated as [37, 38, 78],

$$\Delta G_2(T) = G_2(T) - G_2(0) = -(\varepsilon(T) - 3\,P(T)), \tag{2.7}$$

where $G_2(T)$ denotes the thermal GC, $G_2(0)$, being equal to the condensate value at the deconfinement transition temperature, is the zero temperature condensate value, $\varepsilon(T)$ is the energy density, $P(T)$ is the pressure of the QGP system.

JHEP03(2023)207

To account for the effect of rapidity, one starts from a reference frame where the plasma is at rest and the dipole is moving with a constant velocity so it can be boosted to a reference frame where the dipole is at rest but the plasma is moving past it [49]. Consider a $Q\bar{Q}$ pair moving along x_3 direction with rapidity η. Correspondingly, we can consider a reference frame in which the plasma is at rest and the dipole moves with a constant rapidity $-\eta$ in the x_3 direction. The usual way is to boost the pair into a frame which is at rest while the hot wind of QGP moves against it, so one can consider the following boost to a reference frame in which the dipole is at rest but the plasma is moving past it [49],

$$\begin{aligned} dt &\to dt \cosh\eta - dx_3 \sinh\eta \\ dx_d &\to -dt \sinh\eta + dx_3 \cosh\eta, \end{aligned} \tag{2.8}$$

if we transform the metric (2.3) with (2.8) we obtain,

$$\begin{aligned} ds^2 = \frac{1}{z^2}\Big(& A(z)\, dx_i^2 + [\cosh^2\eta\, A(z) - \sinh^2\eta\, B(z)]\, dx_3^2 - [\cosh^2\eta\, B(z) - \sinh^2\eta\, A(z)]\, dt^2 \\ & - 2[A(z) - B(z)]\, \sinh\eta \cosh\eta\, dx_3\, dt + dz^2\Big), \end{aligned} \tag{2.9}$$

from now on, we can consider the dipole in the gauge theory, which has a gravitational dual with metric (2.9). In continue, we will consider the dipole in two different ways, one transverse to the wind and one parallel to it as,

$$t = \tau, \quad x_1 = \sigma, \quad z = z(\sigma), \quad \text{transverse to the wind,} \tag{2.10}$$

$$t = \tau, \quad x_3 = \sigma, \quad z = z(\sigma), \quad \text{parallel to the wind,} \tag{2.11}$$

remind that in static gauge $z = z(\sigma, \tau) = z(\sigma)$.

2.1 Pair alignment transverse to the wind, Re$V_{Q\bar{Q}}$

Consider the dipole is moving in the x_1 direction that is transverse to the x_3. From (2.10) the spacetime target functions X^μ are $t = \tau$, $x_1 = x = \sigma$, $x_2 = x_3 = constant$,$z(\sigma)$. The heavy $Q\bar{Q}$ potential energy $V_{Q\bar{Q}}$ of this system is related to the expectation value of a rectangular Wilson loop,

$$\langle W(\mathcal{C})\rangle \sim e^{-iS_{str}}, \tag{2.12}$$

S_{str} is the classical Nambu-Goto action of a string in the bulk, so, on the dilaton black hole background, the Nambu-Goto action is given by [42],

$$S_{str} = \frac{1}{2\pi\alpha'} \int d\sigma d\tau e^{\frac{\phi(z)}{2}} \sqrt{-det(G_{\mu\nu}\partial_\alpha X^\mu \partial_\beta X^\nu)}. \tag{2.13}$$

The dilaton factor $e^{\frac{\phi(z)}{2}}$ accounts for the fact that $G_{\mu\nu}$ is the five-dimensional Einstein metric while the target space metric is in the string frame. Therefore, the non-zero coupled dilaton field (2.5) to the background metric (2.3) should be considered when writing the Nambu-Goto action of a test string.

Plugging back S_{str} (2.13) in (2.12) we extract the Re$V_{Q\bar{Q}}$ of $Q\bar{Q}$. Starting from the metric (2.9), dilaton field (2.5), and the spacetime target functions we get,

$$S_{str} = \frac{\mathcal{T}}{2\pi\alpha'}\int_{-L/2}^{L/2} d\sigma\sqrt{f_1(z)\cosh^2\eta - f_2(z)\sinh^2\eta + (f_3(z)\cosh^2\eta - f_4(z)\sinh^2\eta)z'^2(\sigma)}. \tag{2.14}$$

The quarks are located at $x_3 = \frac{L}{2}$ and $x_3 = -\frac{L}{2}$, $z' = \frac{dz}{d\sigma}$ and we defined,

$$\begin{aligned} f_1(z) &= \frac{\omega^2(z)}{z^4}\, A(z)\, B(z), \\ f_2(z) &= \frac{\omega^2(z)}{z^4}\, A^2(z), \\ f_3(z) &= \frac{\omega^2(z)}{z^4}\, B(z), \\ f_4(z) &= \frac{\omega^2(z)}{z^4}\, A(z), \end{aligned} \tag{2.15}$$

and,

$$\omega(z) = e^{\frac{\phi(z)}{2}} = (\frac{1+fz^4}{1-fz^4})^{\frac{c}{f}\sqrt{\frac{3}{8}}}. \tag{2.16}$$

We also write,

$$\begin{aligned} F(z) &= f_1(z)\cosh^2\eta - f_2(z)\sinh^2\eta, \\ G(z) &= f_3(z)\cosh^2\eta - f_4(z)\sinh^2\eta. \end{aligned} \tag{2.17}$$

So action (2.14) could be written as,

$$S_{str} = \frac{\mathcal{T}}{2\pi\alpha'}\int_{-L/2}^{L/2} d\sigma\sqrt{F(z) + G(z)z'^2(\sigma)}. \tag{2.18}$$

The action depends only on $\sigma = x$ and the associated Hamiltonian is a constant of the motion. With the corresponding position of the deepest position in the bulk being z_*, Hamiltonian is,

$$H = \frac{F(z)}{\sqrt{F(z) + G(z)z'^2(\sigma)}} = cte = \sqrt{F(z_*)}. \tag{2.19}$$

From the Hamiltonian (2.19), we can write the equation of motion for $z(x)$ as,

$$\frac{dz}{dx} = \left[\frac{F(z)}{G(z)}\Big(\frac{F(z)}{F(z_*)} - 1\Big)\right]^{\frac{1}{2}}. \tag{2.20}$$

Therefore,

$$dx = \left[\frac{F(z)}{G(z)}\Big(\frac{F(z)}{F(z_*)} - 1\Big)\right]^{-\frac{1}{2}} dz, \tag{2.21}$$

and we can relate L to z_* as follows,

$$\frac{L}{2} = \int_0^{z_*}\left[\frac{F(z)}{G(z)}\Big(\frac{F(z)}{F(z_*)} - 1\Big)\right]^{-\frac{1}{2}} dz. \tag{2.22}$$

JHEP03(2023)207

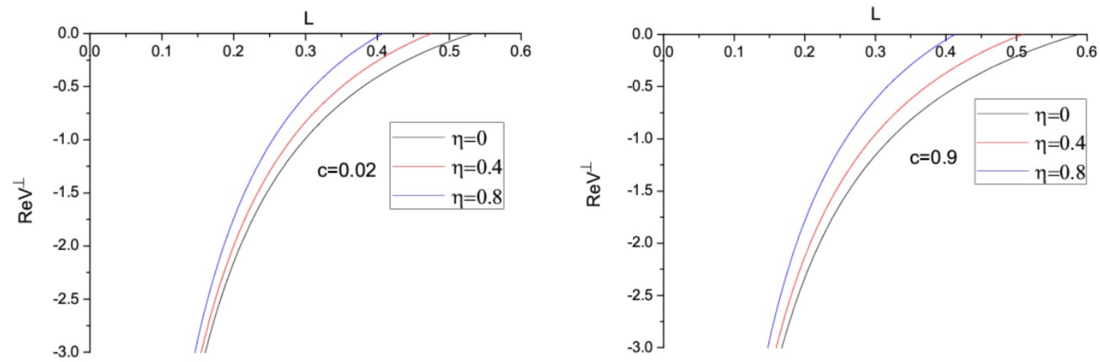

(a) (b)

Figure 1. $\mathrm{Re}\, V_{Q\bar{Q}}$ as a function of L for a $Q\bar{Q}$ pair oriented transverse to the axis of the quarks, from top to bottom for $\eta = 0.8$, 0.4, 0 respectively, $T = 200\, MeV$, in the presence of GC, for a) $c = 0.02$ GeV^4 and b) $c = 0.9$ GeV^4.

From (2.22) we find the length of the line connecting both quarks as,

$$L = 2\sqrt{F(z_*)} \int_0^{z_*} \left[\frac{G(z)}{F(z)(F(z) - F(z_*))}\right]^{\frac{1}{2}} dz. \tag{2.23}$$

In the literature [79, 80] the maximum value of the above length has been used to define a dissociation length for the moving $Q\bar{Q}$ pair, where the dominant configuration for S_{str} is two straight strings (two heavy quarks) running from the boundary to the horizon.

If we put (2.20) in (2.18) the action is written as follows,

$$S_{str} = \frac{\mathcal{T}}{\pi\alpha'} \int_0^{z_*} dz\, \sqrt{G(z)} \sqrt{\frac{F(z)}{F(z_*)}} \left[\frac{F(z)}{F(z_*)} - 1\right]^{-1/2}. \tag{2.24}$$

Note that (2.24) is divergent, which is characteristic of Wilson loops, due to the fact that the string must stretch from the bulk to the boundary in the holographic approach. To regularize the above integral, one can subtract the divergence in S_{str} and obtain the regularized Wilson loop as [48, 49]

$$S^{reg}_{str} = \frac{\mathcal{T}}{\pi\alpha'} \int_0^{z_*} dz\, \sqrt{G(z)} \sqrt{\frac{F(z)}{F(z_*)}} \left[\frac{F(z)}{F(z_*)} - 1\right]^{-1/2} - \frac{\mathcal{T}}{\pi\alpha'} \int_0^{\infty} dz \sqrt{f_3^0(z)}, \tag{2.25}$$

where $f_3^0(z) = f_3(z)\mid_{a\longrightarrow 0}$ (quark self energy). Finally, we proceed from $\mathrm{Re}\, V_{Q\bar{Q}} = S^{reg}_{str}/\mathcal{T}$ to,

$$\mathrm{Re}\, V_{Q\bar{Q}} = \frac{\sqrt{\lambda}}{\pi} \int_0^{z_*} dz\, \sqrt{G(z)} \sqrt{\frac{F(z)}{F(z_*)}} \left[\frac{F(z)}{F(z_*)} - 1\right]^{-1/2} - \frac{\sqrt{\lambda}}{\pi} \int_0^{\infty} dz \sqrt{f_3^0(z)}, \tag{2.26}$$

where $\lambda = \frac{1}{\alpha'^2}$ is the 't Hooft coupling of the gauge theory. Figure 1 shows the $\mathrm{Re}V_{Q\bar{Q}}$ as a function of L with the $Q\bar{Q}$ pair oriented transverse to the axis of the quarks, in the presence of GC. In this figure and all other plots from now on, we consider $T = 200\, MeV$, because at low temperature the heavy quarkonia are hard to dissociate and as the temperature increases the dissociation is more likely to happen [42]. The results show that increasing rapidity leads to a decrease in dissociation length while c has the opposite effect.

JHEP03(2023)207

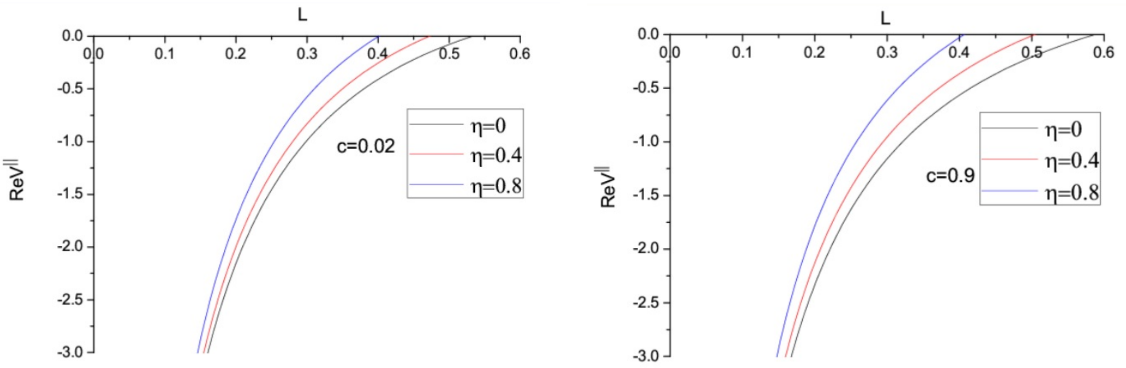

(a) (b)

Figure 2. $\mathrm{Re}\, V_{Q\bar{Q}}$ as a function of L for a $Q\bar{Q}$ pair oriented parallel to the axis of the quarks, from top to bottom for $\eta = 0.8$, 0.4, 0 respectively, $T = 200\, MeV$, in the presence of GC, for a) $c = 0.02$ $\mathrm{Ge}V^4$ and b) $c = 0.9$ $\mathrm{Ge}V^4$.

2.2 Pair alignment parallel to the wind, Re$V_{Q\bar{Q}}$

In this step we consider that the dipole moves parallel to the x_3 direction. From (2.11) the spacetime target functions X^μ are $t = \tau, x_1 = x_2 = constant, x_3 = x = \sigma, z(\sigma)$. Using steps similar to (2.18) we get the action with the new worldsheet as,

$$S_{str} = \frac{\mathcal{T}}{2\pi\alpha'} \int_{-L/2}^{L/2} d\sigma \sqrt{f_1(z) + G(z) z'^2(\sigma)}, \tag{2.27}$$

where $G(z)$ and $f_1(z)$ are defined as (2.17) and (2.15). Similar to the transverse case, we find the line connecting both quarks as,

$$L = 2\sqrt{f_1(z_*)} \int_0^{z_*} \left[\frac{G(z)}{f_1(z)(f_1(z) - f_1(z_*))}\right]^{\frac{1}{2}} dz, \tag{2.28}$$

and the Re$V_{Q\bar{Q}}$ as,

$$\mathrm{Re}\, V_{Q\bar{Q}} = \frac{\sqrt{\lambda}}{\pi} \int_0^{z_*} dz\, \sqrt{G(z)} \sqrt{\frac{f_1(z)}{f_1(z_*)}} \left[\frac{f_1(z)}{f_1(z_*)} - 1\right]^{-1/2} - \frac{\sqrt{\lambda}}{\pi} \int_0^{\infty} dz \sqrt{f_3^0(z)}. \tag{2.29}$$

Figure 2 shows the Re$V_{Q\bar{Q}}$ as a function of LT for some choices of η where $Q\bar{Q}$ pair oriented parallel to the axis of the quarks, in presence of GC. Similar to previous case, increasing rapidity leads to decreasing the dissociation length while c has the opposite effect.

Figure 3 shows a comparison between the Re$V_{Q\bar{Q}}$ for the parallel and the transverse cases. Although the difference is not significant, the plots show that the effect of the GC is slightly stronger for the parallel case. In other words, increasing c increases the dissociation length in both the transverse and the parallel cases (previous figures), this effect appears stronger when the dipole moves parallel to the axis of the quarks.

JHEP03(2023)207

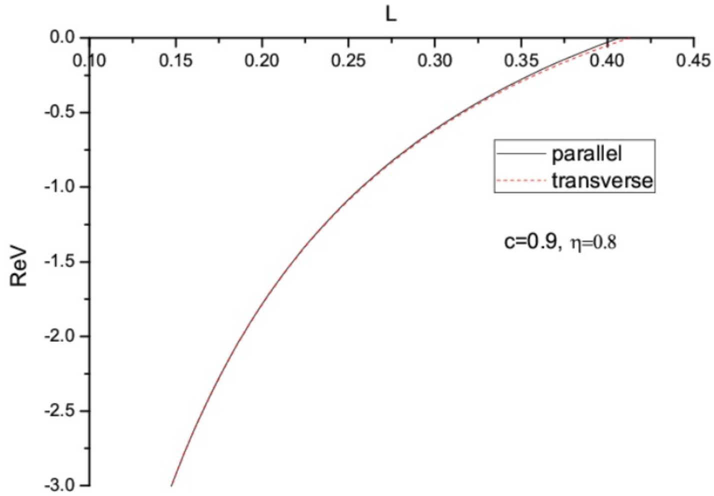

Figure 3. $\mathrm{Re}\,V_{Q\bar{Q}}$ as a function of L, for fixed value of η and fixed value of c, $T = 200\,MeV$, as a comparison between the parallel and the transverse cases. The solid black line shows parallel case and the dashed red line shows transverse case.

3 Imaginary potential of moving $Q\bar{Q}$ in presence of gluon condensation

In this section, we calculate the $\mathrm{Im}V_{Q\bar{Q}}$ using the thermal worldsheet fluctuations method for both the transverse and parallel cases.

3.1 Pair alignment transverse to the wind, $\mathrm{Im}V_{Q\bar{Q}}$

Consider the effect of worldsheet fluctuations around the classical configuration $r = \frac{1}{z}$,

$$r(x) = r_*(x) \to r(x) = r_*(x) + \delta r(x), \tag{3.1}$$

then the fluctuations in the partition function should be considered as follows,

$$Z_{str} \sim \int \mathcal{D}\delta r(x) e^{iS_{NG}(r_*(x)+\delta r(x))}. \tag{3.2}$$

Hence there is an imaginary part of the potential in the action. Dividing the interval of x into $2N$ points (where $N \longrightarrow \infty$) we obtain,

$$Z_{str} \sim \lim_{N\to\infty} \int d[\delta r(x_{-N})] \ldots d[\delta r(x_N)] \exp\left[i\frac{\mathcal{T}\Delta x}{2\pi\alpha'} \sum_j \sqrt{\tilde{G}\, r_j'^2 + \tilde{F}}\right], \tag{3.3}$$

where $\tilde{G}$ and $\tilde{F}$ are functions of r_j. We expand $r_*(x_j)$ around $x = 0$ and keep only terms up to second order of it because thermal fluctuations are important around r_* which means $x = 0$,

$$r_*(x_j) \approx r_* + \frac{x_j^2}{2} r_*''(0), \tag{3.4}$$

considering small fluctuations we have,

$$\tilde{F} \approx \tilde{F}_* + \delta r \tilde{F}_*' + r_*''(0)\tilde{F}_*' \frac{x_j^2}{2} + \frac{\delta r^2}{2}\tilde{F}_*'', \tag{3.5}$$

where $\tilde{F}_* \equiv \tilde{F}(r_*)$ and $\tilde{F}'_* \equiv \tilde{F}'(r_*)$. The action is written as,

$$S_j^{NG} = \frac{\mathcal{T}\Delta x}{2\pi\alpha'}\sqrt{C_1 x_j^2 + C_2}, \tag{3.6}$$

where C_1 and C_2 are given as follows,

$$C_1 = \frac{r_*''(0)}{2}\left[2\tilde{G}_* r_*''(0) + \tilde{F}'_*\right], \tag{3.7}$$

$$C_2 = \tilde{F}_* + \delta r \tilde{F}'_* + \frac{\delta r^2}{2}\tilde{F}''_*, \tag{3.8}$$

to have $ImV_{Q\bar{Q}} \neq 0$, the function in the square root (3.6) should be negative. Then, we consider the j-th contribution to Z_{str} as,

$$I_j \equiv \int_{\delta r_{j\min}}^{\delta r_{j\max}} D(\delta r_j)\,\exp\left[i\frac{\mathcal{T}\Delta x}{2\pi\alpha'}\sqrt{C_1 x_j^2 + C_2}\right], \tag{3.9}$$

$$D(\delta r_j) \equiv C_1 x_j^2 + C_2(\delta r_j), \tag{3.10}$$

$$\delta r = -\frac{\tilde{F}'_*}{\tilde{F}''_*}, \tag{3.11}$$

so, $D(\delta r_j) < 0 \Longrightarrow -x_* < x_j < x_*$ leads to an imaginary part in the square root. We write,

$$x_* = \sqrt{\frac{1}{C_1}\left[\frac{\tilde{F}'^2_*}{2\tilde{F}''_*} - \tilde{F}_*\right]}, \tag{3.12}$$

if the square root is not real we should take $x_* = 0$. With all these conditions we can approximate $D(\delta r)$ by $D(-\frac{\tilde{F}'_*}{\tilde{F}"_*})$ in I_j as,

$$I_j \sim \exp\left[i\frac{\mathcal{T}\Delta x}{2\pi\alpha'}\sqrt{C_1 x_j^2 + \tilde{F}_* - \frac{\tilde{F}'^2_*}{2\tilde{F}''_*}}\right]. \tag{3.13}$$

The total contribution to the imaginary part, will be available with a continuum limit. So,

$$\operatorname{Im} V_{Q\bar{Q}} = -\frac{1}{2\pi\alpha'}\int_{|x|<x_*} dx\sqrt{-x^2 C_1 - \tilde{F}_* + \frac{\tilde{F}'^2_*}{2\tilde{F}''_*}}, \tag{3.14}$$

which leads to,

$$\operatorname{Im} V_{Q\bar{Q}} = -\frac{1}{2\sqrt{2}\alpha'}\sqrt{\tilde{G}_*}\left[\frac{\tilde{F}'_*}{2\tilde{F}''_*} - \frac{\tilde{F}_*}{\tilde{F}'_*}\right]. \tag{3.15}$$

Note that (3.15) is the Im$V_{Q\bar{Q}}$ with the r coordinate. Changing the variable back to the coordinate $z = \frac{1}{r}$ according to our background, we will have,

$$\operatorname{Im} V_{Q\bar{Q}} = -\frac{1}{2\sqrt{2}\alpha'}\sqrt{G_* z_*^2}\left[\frac{F_*}{z_*^2 F'_*} - \frac{z_*^2 F'_*}{4z_*^3 F'_* + 2z_*^4 F''_*}\right], \tag{3.16}$$

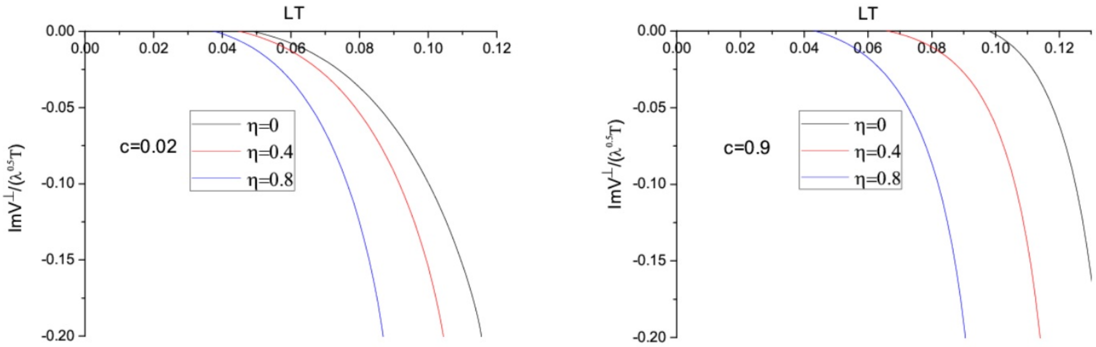

(a) (b)

Figure 4. $\mathrm{Im}V_{Q\bar{Q}}$ as a function of LT for a $Q\bar{Q}$ pair oriented transverse to the axis of the quarks, from left to right for $\eta = 0.8$, 0.4, 0 respectively, $T = 200\,MeV$, in the presence of GC, for a) $c = 0.02$ GeV^4 and b) $c = 0.9$ GeV^4.

where F is again a function of z. In (3.16) the following condition should be satisfied for the square root,

$$\frac{B(z_*)}{A(z_*)} > tanh^2\eta. \tag{3.17}$$

Figure 4 shows the $\mathrm{Im}V_{Q\bar{Q}}$ as a function of LT for some choices of η where $Q\bar{Q}$ pair oriented transverse to the axis of the quarks, in the presence of GC. With increasing rapidity the $\mathrm{Im}V_{Q\bar{Q}}$ is generated for smaller values of LT, implying quarkonium melts more easily, consistent with the results of [81]. Also, by comparing the two panels, one finds c has opposite effects, i.e. by increasing GC, the $\mathrm{Im}V_{Q\bar{Q}}$ is generated for larger distance thus decreasing quarkonium dissociation.

3.2 Pair alignment parallel to the wind, $\mathrm{Im}V_{Q\bar{Q}}$

Taking action (2.27) and using the same approach we followed to find (3.16), we get the $\mathrm{Im}V_{Q\bar{Q}}$ of a pair moving parallel to the axis of the quarks as,

$$\mathrm{Im}\,V_{Q\bar{Q}} = -\frac{1}{2\sqrt{2}\alpha'}\sqrt{G_*}z_*^2\left[\frac{f_{1*}}{z_*^2 f'_{1*}} - \frac{z_*^2 f'_{1*}}{4z_*^3 f'_{1*} + 2z_*^4 f''_{1*}}\right]. \tag{3.18}$$

Figure 5 shows the $\mathrm{Im}V_{Q\bar{Q}}$ as a function of LT for some choices of η where $Q\bar{Q}$ pair oriented parallel to the axis of the quarks, in the presence of GC. Similar to the transverse case, by considering the effect of GC, the $\mathrm{Im}V_{Q\bar{Q}}$ is generated for larger distance thus decreasing quarkonium dissociation, while rapidity has opposite effect. Figure 6 shows a comparison between the $\mathrm{Im}V_{Q\bar{Q}}$ for the parallel and the transverse cases. Similar to $\mathrm{Re}V_{Q\bar{Q}}$ in figure 3, the plots show that the effect of the GC is stronger for the parallel case. While the magnetic field [55] and the chemical potential effects were more important for the transverse case, in the parallel case the GC has a stronger impact.

JHEP03(2023)207

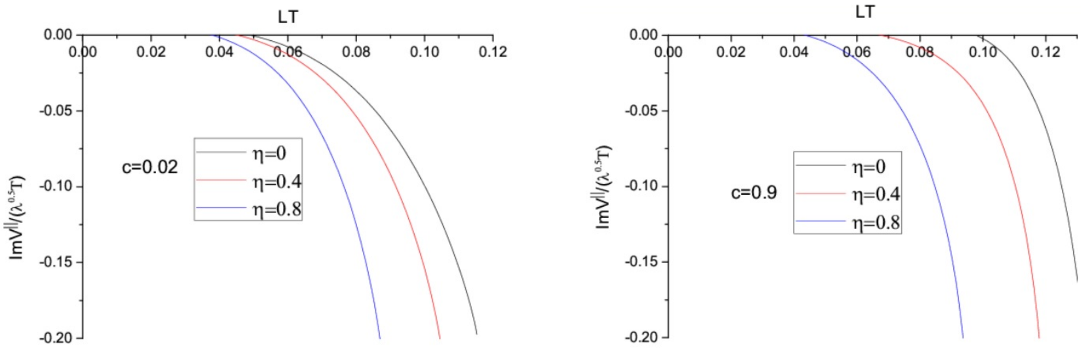

(a) (b)

Figure 5. Im$V_{Q\bar{Q}}$ as a function of LT for a $Q\bar{Q}$ pair oriented parallel to the axis of the quarks, from left to right for $\eta = 0.8$, 0.4, 0 respectively, $T = 200\,MeV$, in the presence of GC, for a) $c = 0.02$ GeV^4 and b) $c = 0.9$ GeV^4.

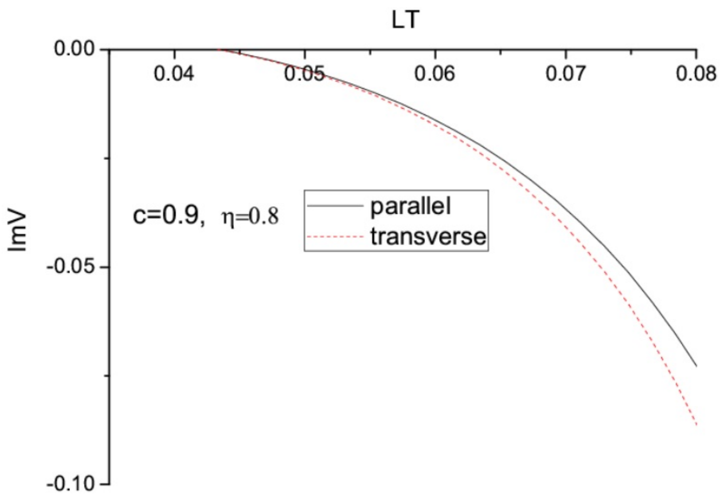

Figure 6. Im$V_{Q\bar{Q}}$ as a function of LT, for fixed value of η and fixed value of c, $T = 200\,MeV$, as a comparison between the parallel and the transverse cases. The (right) black line shows parallel case and the (left) red line shows transverse case.

4 Conclusions

In this work, we investigated the heavy quark potential of a moving $Q\bar{Q}$ pair in a plasma considering the effect of GC. We calculated the Re$V_{Q\bar{Q}}$ and Im$V_{Q\bar{Q}}$ for the cases where the axis of the moving pair is transverse and parallel with respect to its rapidity in the plasma, respectively. For the Re$V_{Q\bar{Q}}$, we used the renormalization scheme proposed in [48, 49] and observed the inclusion of GC decreases Re$V_{Q\bar{Q}}$ and increases the dissociation length, opposite to the effect of the rapidity. For the Im$V_{Q\bar{Q}}$, we adopted the world-sheet thermal fluctuations method [47–49] and found increasing GC, the Im$V_{Q\bar{Q}}$ is generated for larger distance thus decreasing quarkonium dissociation, while rapidity has opposite effect, consistent with the findings of the entropic force [46]. However, we have to admit that the model considered here has a shortcoming: GC is constant implying temperature dependence is absent. An

JHEP03(2023)207

analogous situation happens in [42]. But the existing research, e.g., [43, 44] indicates that the GC appears a drastic change near T_c. In addition, [37] shows that, when T (temperature) is not very high, GC strongly depends on T and μ (chemical potential), and at high temperatures, GC becomes independent of T and μ. From the above analysis, one may infer that as GC decreases in the deconfined phase, Im$V_{Q\bar{Q}}$ is generated for smaller distance thus enhancing quarkonium dissociation, and at high temperatures Im$V_{Q\bar{Q}}$ is nearly not modified by GC. It should be noted that we could not give a concrete conclusion on the Im$V_{Q\bar{Q}}$ at intermediate or low temperatures. To solve this problem we would need to study the competitive effects of GC, μ and T on the Im$V_{Q\bar{Q}}$ and also the correlation among those three. We hope to work on this topic in future.

Acknowledgments

Authors would like to thank Kazem Bitaghsir Fadafan for useful comments. This work was supported by Strategic Priority Research Program of Chinese Academy of Sciences (XDB34030301). Sara Tahery is suppoted by the CAS President International Fellowship Initiative, PIFI (2021PM0065) and Younger Scientist Scholarship (QN2021043004, funding number E11l631KR0).

References

[1] STAR collaboration, *Experimental and theoretical challenges in the search for the quark gluon plasma: The STAR Collaboration's critical assessment of the evidence from RHIC collisions*, *Nucl. Phys. A* **757** (2005) 102 [nucl-ex/0501009] [INSPIRE].

[2] PHENIX collaboration, *Formation of dense partonic matter in relativistic nucleus-nucleus collisions at RHIC: Experimental evaluation by the PHENIX collaboration*, *Nucl. Phys. A* **757** (2005) 184 [nucl-ex/0410003] [INSPIRE].

[3] E.V. Shuryak, *What RHIC experiments and theory tell us about properties of quark-gluon plasma?*, *Nucl. Phys. A* **750** (2005) 64 [hep-ph/0405066] [INSPIRE].

[4] E.V. Shuryak, *Quantum Chromodynamics and the Theory of Superdense Matter*, *Phys. Rept.* **61** (1980) 71 [INSPIRE].

[5] M. Strickland, *Thermal υ_{1s} and chi_b1 suppression in $\sqrt{s_{NN}} = 2.76$ TeV Pb-Pb collisions at the LHC*, *Phys. Rev. Lett.* **107** (2011) 132301 [arXiv:1106.2571] [INSPIRE].

[6] M. Strickland and D. Bazow, *Thermal Bottomonium Suppression at RHIC and LHC*, *Nucl. Phys. A* **879** (2012) 25 [arXiv:1112.2761] [INSPIRE].

[7] M. Margotta et al., *Quarkonium states in a complex-valued potential*, *Phys. Rev. D* **83** (2011) 105019 [*Erratum ibid.* **84** (2011) 069902] [arXiv:1101.4651] [INSPIRE].

[8] G. Aarts et al., *S wave bottomonium states moving in a quark-gluon plasma from lattice NRQCD*, *JHEP* **03** (2013) 084 [arXiv:1210.2903] [INSPIRE].

[9] T. Matsui and H. Satz, *J/ψ Suppression by Quark-Gluon Plasma Formation*, Phys. Lett. B **178** (1986) 416 [INSPIRE].

[10] L. Thakur, N. Haque and H. Mishra, *Heavy quarkonium moving in hot and dense deconfined nuclear matter*, Phys. Rev. D **95** (2017) 036014 [arXiv:1611.04568] [INSPIRE].

[11] N. Brambilla et al., *Heavy Quarkonium in a weakly-coupled quark-gluon plasma below the melting temperature*, JHEP **09** (2010) 038 [arXiv:1007.4156] [INSPIRE].

[12] A. Dumitru, Y. Guo and M. Strickland, *The Imaginary part of the static gluon propagator in an anisotropic (viscous) QCD plasma*, Phys. Rev. D **79** (2009) 114003 [arXiv:0903.4703] [INSPIRE].

[13] M. Laine, O. Philipsen, P. Romatschke and M. Tassler, *Real-time static potential in hot QCD*, JHEP **03** (2007) 054 [hep-ph/0611300] [INSPIRE].

[14] M. Laine, *A Resummed perturbative estimate for the quarkonium spectral function in hot QCD*, JHEP **05** (2007) 028 [arXiv:0704.1720] [INSPIRE].

[15] E. Shuryak, *Why does the quark gluon plasma at RHIC behave as a nearly ideal fluid?*, Prog. Part. Nucl. Phys. **53** (2004) 273 [hep-ph/0312227] [INSPIRE].

[16] S. Borsanyi et al., *Full result for the QCD equation of state with $2+1$ flavors*, Phys. Lett. B **730** (2014) 99 [arXiv:1309.5258] [INSPIRE].

[17] HotQCD collaboration, *Equation of state in $(2+1)$-flavor QCD*, Phys. Rev. D **90** (2014) 094503 [arXiv:1407.6387] [INSPIRE].

[18] A. Rothkopf, T. Hatsuda and S. Sasaki, *Complex Heavy-Quark Potential at Finite Temperature from Lattice QCD*, Phys. Rev. Lett. **108** (2012) 162001 [arXiv:1108.1579] [INSPIRE].

[19] G. Aarts et al., *What happens to the Υ and η_b in the quark-gluon plasma? Bottomonium spectral functions from lattice QCD*, JHEP **11** (2011) 103 [arXiv:1109.4496] [INSPIRE].

[20] G. Aarts et al., *Melting of P wave bottomonium states in the quark-gluon plasma from lattice NRQCD*, JHEP **12** (2013) 064 [arXiv:1310.5467] [INSPIRE].

[21] J.M. Maldacena, *The Large N limit of superconformal field theories and supergravity*, Adv. Theor. Math. Phys. **2** (1998) 231 [hep-th/9711200] [INSPIRE].

[22] E. Witten, *Anti-de Sitter space and holography*, Adv. Theor. Math. Phys. **2** (1998) 253 [hep-th/9802150] [INSPIRE].

[23] P. Kovtun, D.T. Son and A.O. Starinets, *Viscosity in strongly interacting quantum field theories from black hole physics*, Phys. Rev. Lett. **94** (2005) 111601 [hep-th/0405231] [INSPIRE].

[24] G. Policastro, D.T. Son and A.O. Starinets, *The Shear viscosity of strongly coupled $N=4$ supersymmetric Yang-Mills plasma*, Phys. Rev. Lett. **87** (2001) 081601 [hep-th/0104066] [INSPIRE].

[25] J. Erlich, E. Katz, D.T. Son and M.A. Stephanov, *QCD and a holographic model of hadrons*, Phys. Rev. Lett. **95** (2005) 261602 [hep-ph/0501128] [INSPIRE].

[26] L. Da Rold and A. Pomarol, *Chiral symmetry breaking from five dimensional spaces*, Nucl. Phys. B **721** (2005) 79 [hep-ph/0501218] [INSPIRE].

[27] A. Kehagias and K. Sfetsos, *On Running couplings in gauge theories from type IIB supergravity*, Phys. Lett. B **454** (1999) 270 [hep-th/9902125] [INSPIRE].

JHEP03(2023)207

[28] C. Csaki and M. Reece, *Toward a systematic holographic QCD: A Braneless approach*, *JHEP* **05** (2007) 062 [hep-ph/0608266] [INSPIRE].

[29] D. Bak, M. Gutperle, S. Hirano and N. Ohta, *Dilatonic repulsons and confinement via the AdS/CFT correspondence*, *Phys. Rev. D* **70** (2004) 086004 [hep-th/0403249] [INSPIRE].

[30] M.A. Shifman, A.I. Vainshtein and V.I. Zakharov, *QCD and Resonance Physics. Theoretical Foundations*, *Nucl. Phys. B* **147** (1979) 385 [INSPIRE].

[31] Y. Kim, B.-H. Lee, C. Park and S.-J. Sin, *Gluon Condensation at Finite Temperature via AdS/CFT*, *JHEP* **09** (2007) 105 [hep-th/0702131] [INSPIRE].

[32] S.H. Lee, *Gluon condensates above* T_c, *Phys. Rev. D* **40** (1989) 2484 [INSPIRE].

[33] M. D'Elia, A. Di Giacomo and E. Meggiolaro, *Gauge invariant field strength correlators in pure Yang-Mills and full QCD at finite temperature*, *Phys. Rev. D* **67** (2003) 114504 [hep-lat/0205018] [INSPIRE].

[34] D.E. Miller, *Lattice QCD Calculation for the Physical Equation of State*, *Phys. Rept.* **443** (2007) 55 [hep-ph/0608234] [INSPIRE].

[35] R. Carcasses Quevedo, J.L. Goity and R. Trinchero, *QCD condensates and holographic Wilson loops for asymptotically AdS spaces*, *Phys. Rev. D* **89** (2014) 036004 [arXiv:1311.1175] [INSPIRE].

[36] S. Nojiri and S.D. Odintsov, *Two boundaries AdS/CFT correspondence in dilatonic gravity*, *Phys. Lett. B* **449** (1999) 39 [hep-th/9812017] [INSPIRE].

[37] P. Colangelo, F. Giannuzzi, S. Nicotri and F. Zuo, *Temperature and chemical potential dependence of the gluon condensate: a holographic study*, *Phys. Rev. D* **88** (2013) 115011 [arXiv:1308.0489] [INSPIRE].

[38] P. Castorina and M. Mannarelli, *Effective degrees of freedom and gluon condensation in the high temperature deconfined phase*, *Phys. Rev. C* **75** (2007) 054901 [hep-ph/0701206] [INSPIRE].

[39] P.N. Kopnin and A. Krikun, *Wilson loops in holographic models with a gluon condensate*, *Phys. Rev. D* **84** (2011) 066002 [arXiv:1106.4978] [INSPIRE].

[40] X. Chen, D. Li and M. Huang, *Criticality of QCD in a holographic QCD model with critical end point*, *Chin. Phys. C* **43** (2019) 023105 [arXiv:1810.02136] [INSPIRE].

[41] G.E. Brown, J.W. Holt, C.-H. Lee and M. Rho, *Late Hadronization and Matter Formed at RHIC: Vector Manifestation, Brown-Rho Scaling and Hadronic Freedom*, *Phys. Rept.* **439** (2007) 161 [nucl-th/0608023] [INSPIRE].

[42] Y. Kim, B.-H. Lee, C. Park and S.-J. Sin, *The Effect of gluon condensate on holographic heavy quark potential*, *Phys. Rev. D* **80** (2009) 105016 [arXiv:0808.1143] [INSPIRE].

[43] G. Boyd et al., *Thermodynamics of* SU(3) *lattice gauge theory*, *Nucl. Phys. B* **469** (1996) 419 [hep-lat/9602007] [INSPIRE].

[44] G. Boyd and D.E. Miller, *The Temperature dependence of the* $\mathrm{SU}(N)$ *gluon condensate from lattice gauge theory*, hep-ph/9608482 [BI-TP-96-28] [INSPIRE].

[45] Z.-Q. Zhang and X. Zhu, *Effect of gluon condensate on jet quenching parameter and drag force*, *Eur. Phys. J. C* **79** (2019) 107 [INSPIRE].

[46] Z.-Q. Zhang and D.-F. Hou, *Entropic destruction of heavy quarkonium in quark-gluon plasma with gluon condensate*, *Phys. Lett. B* **803** (2020) 135301 [INSPIRE].

[47] J. Noronha and A. Dumitru, *Thermal Width of the Υ at Large t' Hooft Coupling*, *Phys. Rev. Lett.* **103** (2009) 152304 [arXiv:0907.3062] [INSPIRE].

[48] S.I. Finazzo and J. Noronha, *Estimates for the Thermal Width of Heavy Quarkonia in Strongly Coupled Plasmas from Holography*, *JHEP* **11** (2013) 042 [arXiv:1306.2613] [INSPIRE].

[49] S.I. Finazzo and J. Noronha, *Thermal suppression of moving heavy quark pairs in a strongly coupled plasma*, *JHEP* **01** (2015) 051 [arXiv:1406.2683] [INSPIRE].

[50] Q.J. Ejaz et al., *A Limiting velocity for quarkonium propagation in a strongly coupled plasma via AdS/CFT*, *JHEP* **04** (2008) 089 [arXiv:0712.0590] [INSPIRE].

[51] B.K. Patra, H. Khanchandani and L. Thakur, *Velocity-induced Heavy Quarkonium Dissociation using the gauge-gravity correspondence*, *Phys. Rev. D* **92** (2015) 085034 [arXiv:1504.05396] [INSPIRE].

[52] A. Saha and S. Gangopadhyay, *Holographic computation of Wilson loops in a background with broken conformal invariance and finite chemical potential*, *Phys. Rev. D* **101** (2020) 086022 [arXiv:1912.05940] [INSPIRE].

[53] M. Ali-Akbari, D. Giataganas and Z. Rezaei, *Imaginary potential of heavy quarkonia moving in strongly coupled plasma*, *Phys. Rev. D* **90** (2014) 086001 [arXiv:1406.1994] [INSPIRE].

[54] J. Sadeghi and S. Tahery, *The effects of deformation parameter on thermal width of moving quarkonia in plasma*, *JHEP* **06** (2015) 204 [arXiv:1412.8332] [INSPIRE].

[55] Z.-Q. Zhang and D.-F. Hou, *Imaginary potential in strongly coupled $\mathcal{N} = 4$ SYM plasma in a magnetic field*, *Phys. Lett. B* **778** (2018) 227 [arXiv:1802.01919] [INSPIRE].

[56] S. Tahery and J. Sadeghi, *The investigation of quark-antiquark potential in a plasma with hyperscaling violation background*, *J. Phys. G* **44** (2017) 105001 [arXiv:1509.01309] [INSPIRE].

[57] Y.-Q. Zhao, Z.-R. Zhu and X. Chen, *The effect of gluon condensate on imaginary potential and thermal width from holography*, *Eur. Phys. J. A* **56** (2020) 57 [arXiv:1909.04994] [INSPIRE].

[58] J.L. Albacete, Y.V. Kovchegov and A. Taliotis, *Heavy Quark Potential at Finite Temperature in AdS/CFT Revisited*, *Phys. Rev. D* **78** (2008) 115007 [arXiv:0807.4747] [INSPIRE].

[59] K. Bitaghsir Fadafan, D. Giataganas and H. Soltanpanahi, *The Imaginary Part of the Static Potential in Strongly Coupled Anisotropic Plasma*, *JHEP* **11** (2013) 107 [arXiv:1306.2929] [INSPIRE].

[60] K.B. Fadafan and S.K. Tabatabaei, *Thermal Width of Quarkonium from Holography*, *Eur. Phys. J. C* **74** (2014) 2842 [arXiv:1308.3971] [INSPIRE].

[61] K. B. Fadafan and S.K. Tabatabaei, *The Imaginary Potential and Thermal Width of Moving Quarkonium from Holography*, *J. Phys. G* **43** (2016) 095001 [arXiv:1501.00439] [INSPIRE].

[62] N.R.F. Braga and L.F. Ferreira, *Thermal width of heavy quarkonia from an AdS/QCD model*, *Phys. Rev. D* **94** (2016) 094019 [arXiv:1606.09535] [INSPIRE].

[63] G.F. de Teramond and S.J. Brodsky, *Hadronic spectrum of a holographic dual of QCD*, *Phys. Rev. Lett.* **94** (2005) 201601 [hep-th/0501022] [INSPIRE].

[64] Y. Kim, J.-P. Lee and S.H. Lee, *Heavy quarkonium in a holographic QCD model*, *Phys. Rev. D* **75** (2007) 114008 [hep-ph/0703172] [INSPIRE].

[65] M.Á. Escobedo, *The relation between cross-section, decay width and imaginary potential of heavy quarkonium in a quark-gluon plasma*, J. Phys. Conf. Ser. **503** (2014) 012026 [arXiv:1401.4892] [INSPIRE].

[66] S.-Q. Feng, Y.-Q. Zhao and X. Chen, *Systematical study of thermal width of heavy quarkonia in a finite temperature magnetized background from holography*, Phys. Rev. D **101** (2020) 026023 [arXiv:1910.05668] [INSPIRE].

[67] T. Hayata, K. Nawa and T. Hatsuda, *Time-dependent heavy-quark potential at finite temperature from gauge-gravity duality*, Phys. Rev. D **87** (2013) 101901 [arXiv:1211.4942] [INSPIRE].

[68] Y. Burnier, M. Laine and M. Vepsalainen, *Quarkonium dissociation in the presence of a small momentum space anisotropy*, Phys. Lett. B **678** (2009) 86 [arXiv:0903.3467] [INSPIRE].

[69] D. Dudal and T.G. Mertens, *Melting of charmonium in a magnetic field from an effective AdS/QCD model*, Phys. Rev. D **91** (2015) 086002 [arXiv:1410.3297] [INSPIRE].

[70] N.R.F. Braga and L.F. Ferreira, *Heavy meson dissociation in a plasma with magnetic fields*, Phys. Lett. B **783** (2018) 186 [arXiv:1802.02084] [INSPIRE].

[71] L. Bellantuono et al., *Quarkonium dissociation in strongly coupled far-from-equilibrium matter: holographic description*, Nucl. Phys. A **982** (2019) 931 [INSPIRE].

[72] L. Bellantuono et al., *Quarkonium dissociation in a far-from-equilibrium holographic setup*, Phys. Rev. D **96** (2017) 034031 [arXiv:1706.04809] [INSPIRE].

[73] M.A. Escobedo, F. Giannuzzi, M. Mannarelli and J. Soto, *Heavy Quarkonium moving in a Quark-Gluon Plasma*, Phys. Rev. D **87** (2013) 114005 [arXiv:1304.4087] [INSPIRE].

[74] K.G. Wilson, *Confinement of Quarks*, Phys. Rev. D **10** (1974) 2445 [INSPIRE].

[75] J.-L. Gervais and A. Neveu, *The Slope of the Leading Regge Trajectory in Quantum Chromodynamics*, Nucl. Phys. B **163** (1980) 189 [INSPIRE].

[76] A.M. Polyakov, *Gauge Fields as Rings of Glue*, Nucl. Phys. B **164** (1980) 171 [INSPIRE].

[77] U. Gursoy, E. Kiritsis and F. Nitti, *Exploring improved holographic theories for QCD: Part II*, JHEP **02** (2008) 019 [arXiv:0707.1349] [INSPIRE].

[78] P.M. Zerwas and H.A. Kastrup, *Workshop on QCD: 20 Years Later* Aachen Germany, June 9–13 1992 [World Scientific, New Jersey (1993)] [INSPIRE].

[79] H. Liu, K. Rajagopal and U.A. Wiedemann, *An AdS/CFT Calculation of Screening in a Hot Wind*, Phys. Rev. Lett. **98** (2007) 182301 [hep-ph/0607062] [INSPIRE].

[80] H. Liu, K. Rajagopal and U.A. Wiedemann, *Wilson loops in heavy ion collisions and their calculation in AdS/CFT*, JHEP **03** (2007) 066 [hep-ph/0612168] [INSPIRE].

[81] K. B. Fadafan and S.K. Tabatabaei, *Entropic destruction of a moving heavy quarkonium*, Phys. Rev. D **94** (2016) 026007 [arXiv:1512.08254] [INSPIRE].

JHEP03(2023)207